Article

# First-Principles Insights into Structural, Optoelectronic, and Elastic Properties of Fluoro-Perovskites KXF$_3$ (X = Ru, Os)

Jehan Y. Al-Humaidi, Javed Iqbal,* Abdullah, Naimat Ullah Khan, Shagufta Rasool, Ali Algahtani, Vineet Tirth, Altaf Ur Rahman, Barno Sayfutdinovna Abdullaeva, Moamen S. Refat, Muhammad Aslam, and Abid Zaman*
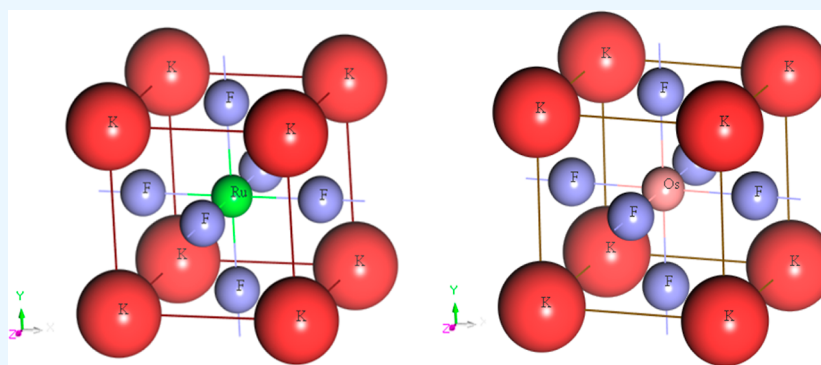
Read Online

ACCESS | Metrics & More | Article Recommendations

**ABSTRACT:** The need for new and better semiconductor materials for use in renewable energy devices motivates us to study KRuF$_3$ and KOsF$_3$ fluoride materials. In the present work, we computationally studied these materials and elaborate their varied properties comprehensively with the assistance of density functional theory-based techniques. To find the structural stability of these under-consideration materials, we employed the Birch−Murnaghan fit, while their electronic characteristics were determined with the usage of modified potential of Becke−Johnson. During the study, it became evident from the band-structure results of the KRuF$_3$ and KOsF$_3$ materials that both present an indirect semiconductor nature having the band gap values of 2.1 and 1.7 eV, respectively. For both the studied materials, the three essential elastic constants were determined first, which were further used to evaluate all the mechanical parameters of the studied materials. From the calculated values of Pugh's ratio and Poisson's ratio for the KRuF$_3$ and KOsF$_3$ materials, both were verified to procure the nature of ductility. During the study, we concluded from the results of absorption coefficient and optical conduction in the UV energy range that both the studied materials proved their ability for utilization in the numerous future optoelectronic devices.

## INTRODUCTION

The world is advancing in each aspect of life, but nowadays challenging situations are developed due to the fear of falling the shortage of nonrenewable resources in future. This fear motivated researchers to find some other ways that can facilitate humans in the same or even in much better way. This craze eventually brought the researchers to new turn/stage, and some other materials have been developed that work on renewable energy rather than the nonrenewable energy. Among those developed materials, ABX$_3$ materials have much attracted the research community toward itself due to their special properties. During the past few decades, researchers reported numerous such kinds of ABX$_3$ materials having a similar structure to that of calcium titanate, and those materials have been employed in uncountable modern practical applications by the engineers. On the basis of their

extraordinary properties displayed by these ABX$_3$ materials, they are preferred for their enforcement in devices like: photovoltaic cells, photovoltaic electrodes, LED's, energy storage devices, temperatures detectors, numerous gases sensor, wireless communications systems, for negligible resistance conducting devices, lasers, and various other sort of applications.[1−11]

In the ABX$_3$ formula having a cubic perovskite structure, when fluorine is placed at position X, then it is known as a
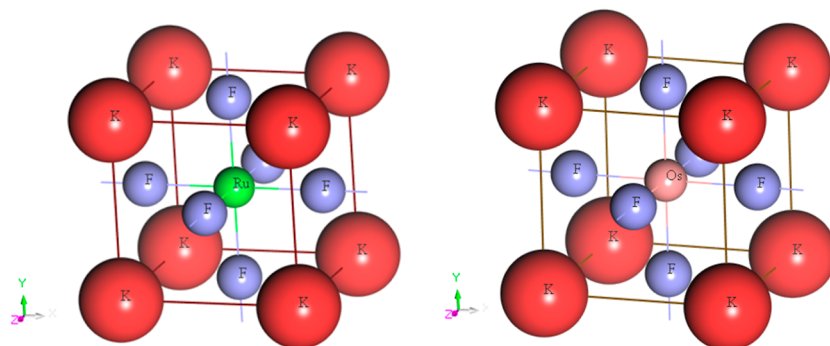
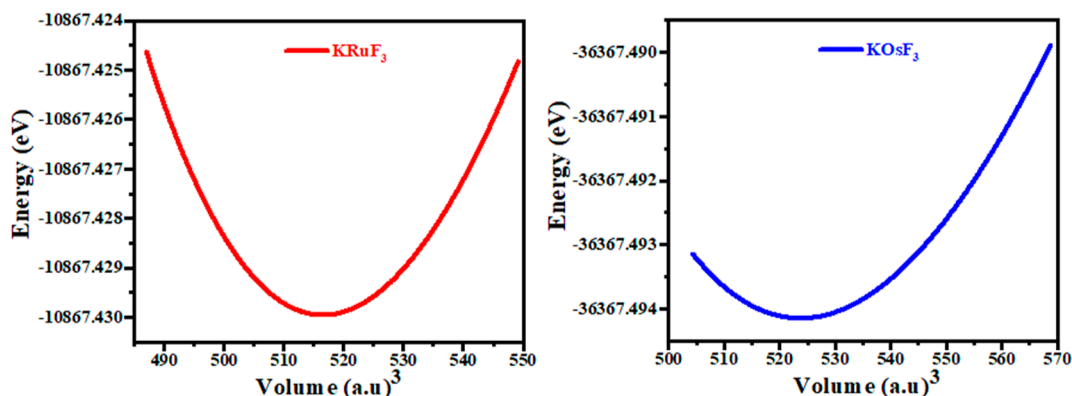**Figure 1.** Unit cell structure of KXF$_3$ (X = Ru and Os). .



**Figure 2.** Optimized energy and volume curve of the KXF$_3$ (X = Ru and Os) materials. .

fluoride perovskite material. These fluoride perovskite materials took a great interest in the modern industries especially semiconductor industries due to their specific properties because of having large band gaps. These materials have been implemented in various applications like: high temperature superconductors, gigabit memory, photovoltaic, piezo-electric devices, colossal magneto-resistance appliances, photo luminescence, etc.,[12−17] Due to their need for such types of appliances, huge amounts of fluoride materials have been searched and reported by the researcher's community both experimentally and computationally. In 2019, a researcher reported a group of fluoride AVF$_3$ (A = K, Rb, and Na) materials and on the basis of the optical and thermal properties possessed by these fluoride materials, the author argued for their usage in optoelectronic and thermoelectric devices.[18] Recently, another group investigated MTiF$_3$ materials and studied their properties deeply. The authors found that these materials are stable in the cubic structure and have a ductile nature. During the study of these materials, it was found that these materials have dual nature of conducting and non-conducting in their spin up and spin down, respectively.[19] Similarly, Chenine et al. studied theoretically the behavior of NaXF$_3$ (X = V, Co) compounds and reported that these materials have perovskite structures. They reported that these materials are mechanically stable and possess good thermal and magnetic properties.[20]

Looking into the potential applications of Halide perovskites in modern technology, we have been prompted to conduct a full-fledged study and explore the electronic, structural, elastic, and optical properties of KXF$_3$ (X = Ru and Os) which are still under cover. Since Ru and Os both have smaller ionic radii than the K (which is placed at A-site) and can be adjusted at B-

site in the compound. To accomplish the study, Tran and Blaha modified Becke-gradient potential has been used, as these are generally efficient in calculating most properties under the framework of density functional theory (DFT). This theoretical work will gather information regarding these crucial compounds and in future this study can be used as a reference for experimentalists and theoreticians.

## ■ RESULTS AND DISCUSSION

**Structural Properties.** The structures of both studied KRuF$_3$ and KOsF$_3$ having cubic phases are shown in Figure 1. The studied materials have similar structure to that of ABX$_3$; with K at the A site, Ru/OS at the B site, and fluorine at the X site having a space group of pm-3m (221). As it is clear from the Figure 1, that K have coordinates of (0, 0, 0), Ru/Os reside in the center of cube having the coordinates of (0.5, 0.5, 0.5), and last fluorine is placed on each face of the cube with the coordinates of (0, 0.5, 0.5). Meanwhile, all the other information about their structures were collected from their respective volume and energy curves, as shown in Figure 2. The lattice constants measured for the KRuF$_3$ and KOsF$_3$ materials were found to have slight differences with each other with values of 4.24 and 4.26 Å, respectively. As a result, the KOsF$_3$ also had a higher value of volume at the ground state, as shown in Table 1. From Figure 2, it is clear that the KRuF$_3$ material procures the minimal value of energy at ground state (−10 867.4 Ry) than the KOsF$_3$ and hence strengthens its capability to be more stable in cubic structure than the KOsF$_3$ material. However, the bulk modulus was recorded as 85.3 for the KOsF$_3$ compound, which is greater than that of the KRuF$_3$ compound (82.4). Moreover, in order to further ensure the stability of KRuF$_3$ and KOsF$_3$ compounds in the cubic

**Table 1. Computed Structural Parameters of KXF₃ (X = Ru and Os)**

| structural parameters | KRuF₃ | KOsF₃ |
|---|---|---|
| equilibrium lattice constant $(a_o)$ | 4.24 | 4.26 |
| bulk modulus $(B_0)$ | 82.4 | 85.3 |
| ground state volume $(V_0)$ | 516.5 | 523.4 |
| bulk modulus first derivative $B'$ | 5 | 5 |
| energy at ground state $(E_0)$ | −10 867.4 | −36 367.4 |
| tolerance factor | 0.96 | 0.95 |
| octahedral factor | 0.54 | 0.52 |
| formation Energy (eV) | −3.6 | −2.5 |

structure, the Gold-Schmidt tolerance factors $(\tau)$ were also calculated and are listed in Table 1. Both materials showed the Gold-schmidt tolerance factor $(\tau)$ values in the range (i.e., 0.8 to 1), as demanded for stability of the cubic perovskite structures.[21] Since both KRuF₃ and KOsF₃ materials have cubic perovskite structures, it is essential that their octahedral factor $(\mu)$ values must be greater than 0.44 and less than 0.90. As shown in the Table 1, both the studied materials fulfill the condition of octahedral factor.[21] In order to determine the possibility of synthesizing these materials, their formation energies were computed using the formula

$$E_{FE} = E_{KXF3} - (E_K + E_X + 3E_F)$$

The calculated values are presented in Table 1. The negative values of the formation energies show that these materials can be synthesized.[22]

**Phonon Spectra.** For the fabrication of a real device, material stability is very important. To see the potential applications of KRuF₃ and KOsF₃, we have carried out the phonon dispersion to check their stability. KRuF₃ and RuOsF₃ perovskite compounds are structurally stable, as can be observed in Figure 3. We have looked into the dynamic stability of KRuF₃ and RuOsF₃ perovskite compounds at equilibrium lattice constant using Phonopy code.[23] The dynamic stability of the perovskite materials KRuF₃ and RuOsF₃ is revealed by the phonon spectrum at the equilibrium lattice constant. The computed phonon band structure shows that KRuF3 and RuOsF₃ perovskite compounds are kinetically stable. Our results are an analogy to RbXF₃ (X = Ir, Os, and Rh) and other previous studies.[24,25]

**Electronic Properties.** The electronic properties, of the compounds facilitate researchers to know about their nature and also provide enough information to forecast about the properties, which a material will display. In the present approach, TB-mBJ approximation was employed to analyze the band-structures, total density of states (TDOS), and partial

density of states (PDOS) of the studied compounds, while their results are illustrated in Figure 4a,b It is evident from the
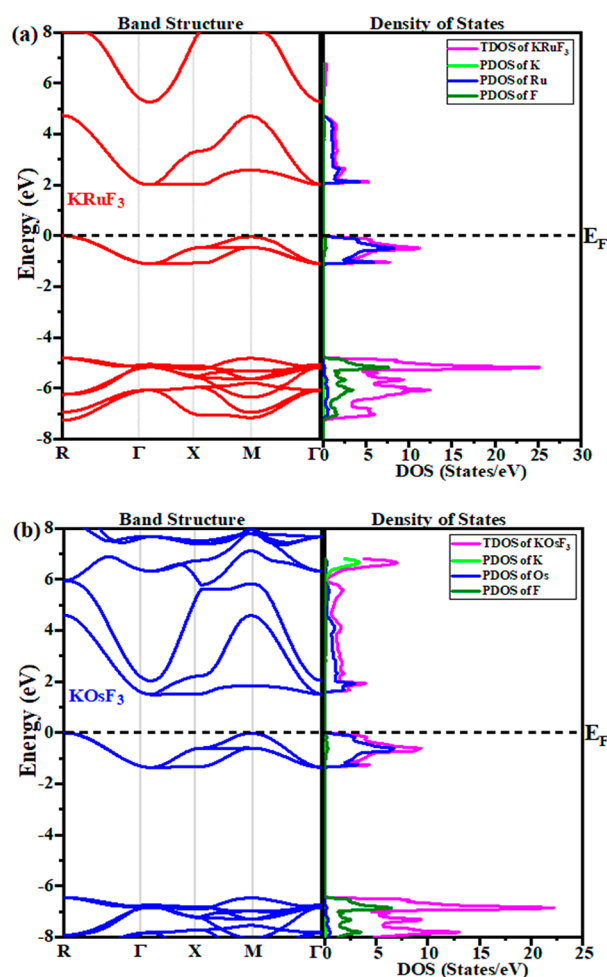


**Figure 4.** Electronic band structures with the predicted TDOS and PDOS for (a) KRuF₃ and (b) KOsF₃ compounds. .

band-structures results of the KRuF₃ and KOsF₃ materials that both present indirect band gaps having the values of 2.1 and 1.7 eV, respectively. Owing to a large band gap between the valence and conduction bands of the KRuF₃ material, the electrons in the KRuF₃ material valence band will require more energy for its thermal excitation to become conduction electrons than the KOsF₃ material valence electrons. Since none of the bands (i.e., conduction and valence) overlaps the zero value which is the Fermi level, this conduction of these
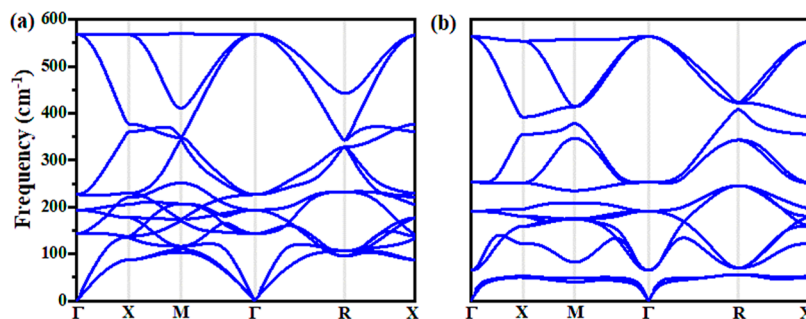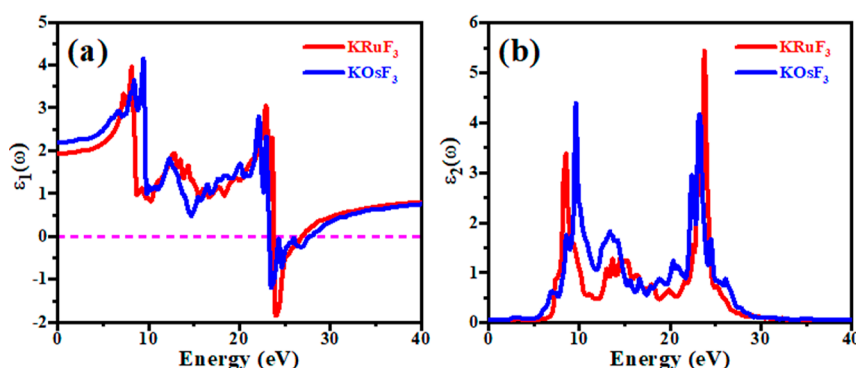


**Figure 3.** Calculated phonon dispersion curves of (a) KRuF₃ and (b) KOsF₃. .

**Table 2. Computed Elastic Parameters of KXF$_3$ (X = Ru and Os)**

| compounds | $C_{11}$ (GPa) | $C_{12}$ (GPa) | $C_{44}$ (GPa) | $B$ (GPa) | $A$ | $G$ (GPa) | $E$ (GPa) | $V$ | $B/G$ |
|---|---|---|---|---|---|---|---|---|---|
| **KRuF$_3$** | 155.2 | 43.6 | 6.5 | 80.33 | 0.1 | 8.3 | 24.1 | 0.66 | 9.68 |
| **KOsF$_3$** | 137.5 | 65.7 | 14.6 | 89.4 | 0.4 | 1.9 | 5.7 | 0.73 | 46.53 |



**Figure 5.** Dielectric function of (a) real part and (b) imaginary part of the KXF$_3$ (X = Ru and Os). .

two materials manifest them of having semiconducting nature, as shown in Figure 4a,b.

Moreover, the TDOS (contribution of PDOS of its all components) and PDOS (subshell contribution of each atom) were also determined for both the materials, as presented in Figure 4a,b. It is clear from the results of the TDOS and PDOS for both the materials that none of the curve exceeds the zero level (Fermi level) and hence both materials have semiconducting nature as predicted from the results of bandstructures of both the materials. It is also evident from Figure 4a,b that the PDOS of fluorine (especially PDOS of the p-state) atom has greater contribution in the TDOS of both materials in their valence bands. Furthermore, from the TDOS and PDOS patterns, it also became clarified that the separation between the valence and conduction bands curves of the KRuF$_3$ and KOsF$_3$ materials is exactly the same (i.e., 2.1 eV for KRuF$_3$, while 1.7 eV for KOsF$_3$) as calculated from the bandstructures of these two materials.

**Elastic Properties.** The mechanical properties of any material show its capability to withstand the external applied load. So, it is obligatory to determine the mechanical conduct of any material before its enforcement in any practical device. For the above said purpose, we determine the mechanical properties of KRuF$_3$ and KOsF$_3$ materials and their respective values of each mechanical property are given in Table 2. From the Table 2, it is clear that all the essential requirements, (1) $C_{11} - C_{12} > 0$, (2) $2C_{12} + C_{11} > 0$, and (3) $C_{11}$ and $C_{44} > 0$, of mechanical stability have been fulfilled by the calculated elastic constants for both the materials.[26] From the mechanical results of the presently studied materials, it is clear that the KOsF$_3$ material has a greater bulk modulus ($B$) value of 89.4 N/m$^2$ than the KRuF$_3$, so it became evident that for the same compressive force, the KRuF$_3$ material will show less resistance to the uniform compression. Nevertheless, the values of the $E$ and $G$ were found greater for the KRuF$_3$ material than the KOsF$_3$ material. These values of $E$ and $G$ for the KRuF$_3$ material ensure its immense elasticity ability and higher capacity of resistance to the shearing deformation, respectively, than the KOsF$_3$ material. Moreover, both materials were observed to have anisotropic nature because their calculated values of anisotropic factor ($A$) were not equal to 1 (i.e., which is need for isotropic materials).[27] Finally, Poisson's ratio ($V$)

and $B/G$ ratio were calculated for both KRuF$_3$ and KOsF$_3$ materials for the declaration of their ductility and brittleness behavior. For ductile material, it is necessary that the values of $V$ & $B/G$ ratio must be higher than 0.33 and 1.75, respectively.[19] From the calculated values of $B/G$ ratio and $V$ for the KRuF$_3$ and KOsF$_3$ materials given in Table 2, both were verified to procure the nature of ductility.

**Optical Properties.** *Dielectric Function.* The dielectric function (which comprised two parts, i.e., real and imaginary) of both the studied KRuF$_3$ and KOsF$_3$ materials are illustrated in Figure 5. It is imperative to elaborate the dielectric function while studying the optical properties of any material because it determines how the incident photons interact with the material when they fall on them. The information about the degree of polarization and how the electromagnetic waves are dispersed when they enter the material is demonstrated by the real part of the dielectric function. The static values of $\varepsilon_1(\omega)$ for both the KRuF$_3$ and KOsF$_3$ materials as shown in Figure 5, were noted as 1.9 and 2.2, respectively. However, with the initial increment in the energy both the $\varepsilon_1(\omega)$ curves of the KRuF$_3$ and KOsF$_3$ materials showed improvement in their values and acquired their maximum value of 4 and 4.3 at energy values of 7 and 9, respectively. However, after achieving their maximum values, both the materials showed a sudden degradation in their $\varepsilon_1(\omega)$ values with a minor increase in the energy. Afterward, the curves of the $\varepsilon_1(\omega)$ for both the materials showed a random manner of variation in their values in the range of 0.5−2.5 until the energy reaches to 22.5 eV. At energy values of 24 and 23.8 eV, both the KRuF$_3$ and KOsF$_3$ materials achieved negative values of $\varepsilon_1(\omega)$, respectively. It means that, at these values of energy (i.e., 24 and 23.8 eV) both materials showed a metallic nature and will reflect all the incident photons fall upon them.[28] The imaginary parts of KRuF$_3$ and KOsF$_3$ materials are also presented in Figure 5. From the figure, it is clear that above the 5 eV both the KRuF$_3$ and KOsF$_3$ materials acquire the effective enhancement in their $\varepsilon_2(\omega)$ values and obtained their last highest peaks in the energy range of 22−24 eV. The first peak of $\varepsilon_2(\omega)$ spectra is closely related to the optical band gap which is the threshold for optical transition between valence band maximum and conduction band minimum. The optical band gap is related with the electronic band gap.[29] This part of the dielectric
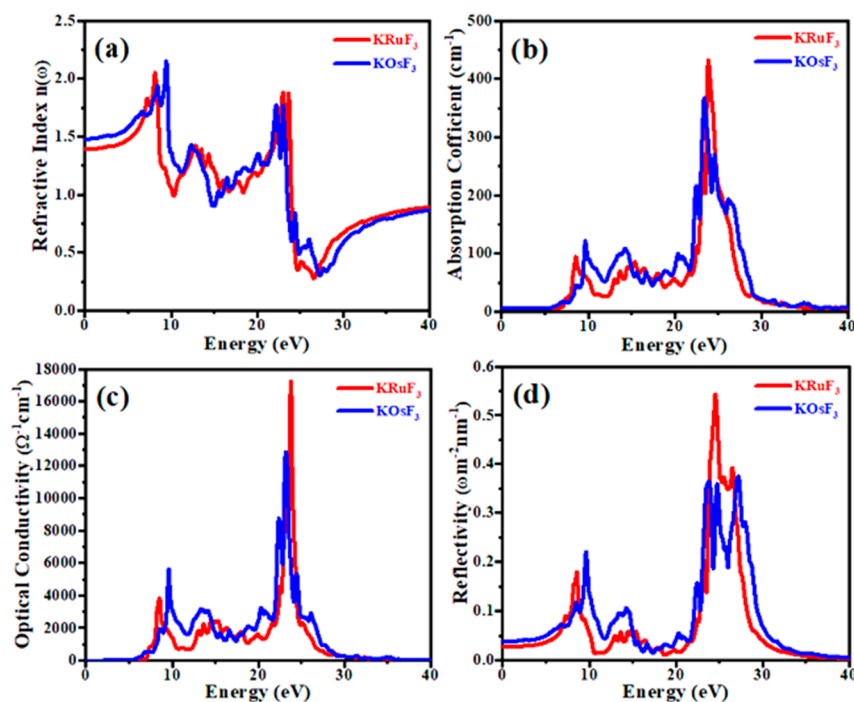
**Figure 6.** Optical parameters: (a) refractive index, (b) absorption coefficient, (c) optical conductivity, and (d) reflectivity of the $KXF_3$ (X = Ru and Os). .

function enables the material engineers for selecting any material for practical application because the absorption ability of any material can be premeditated from $\varepsilon_2 (\omega)$.[30]

*Refractive Index.* The refractive index curves in the energy range of 0−40 eV were plotted for $KRuF_3$ and $KOsF_3$ materials and are shown in Figure 6. The static values of refractive index were noted as 1.4 and 1.48 for $KRuF_3$ and $KOsF_3$ materials, respectively. It is clear from the noted static values of $\varepsilon_1(\omega)$ and refractive index for the $KRuF_3$ and $KOsF_3$ compounds that they have satisfied the condition of $\varepsilon_1(0) = n^2(0)$.[18] Moreover, their curves {i.e., refractive index and $\varepsilon_1(\omega)$} showed similar manner of fluctuation with the energy, as shown in Figures 5a and 6a. In the energy range of 20−24 eV the $KRuF_3$ material showed a higher value of refractive index than the $KOsF_3$ material, which means that the incident photons experience more retardation in the $KRuF_3$ material than the $KOsF_3$ material in this range of energy.

*Absorption Coefficient.* For the presently studied materials, their curves of absorption coefficients in the energy range of 0−40 eV are displayed in Figure 6b. From the figure, it is obvious that both the materials did not gave response of absorption to low energy photons, but as the energy was slightly raised from 6 eV, the $KOsF_3$ material showed first its absorbing response. Meanwhile, the $KRuF_3$ material showed its capability of absorption to the incident photons having higher energy than 7 eV in the UV range. For the later enhancement in the photon's energy than their first response of absorbing photons, both the materials showed variation in their absorption values. Both $KRuF_3$ and $KOsF_3$ materials were detected to have higher (i.e., 420 and 360) values of absorption for the incident photons having the UV energies of 23.8 eV− 24.2 eV. Moreover, $KRuF_3$ compounds showed its greater response of absorption than the $KOsF_3$ compound. However, for the further increment in the photon energy, both materials showed a continuous decline in their curves of absorption.

*Optical Conductivity.* The optical conductivity of any material is totally dependent on its absorbing quality of photons. The optical conductivities of $KRuF_3$ and $KOsF_3$ materials were also determined and illustrated in Figure 6c. From Figure 6b,c, it is clear that both the curves of the optical conductivity and absorption coefficient have the same manner of raising and falling with the photon's energy variation. From Figure 6c, it is clear that the $KOsF_3$ material showed first improvement in its optical conductivity to the incident photons compared to the $KRuF_3$ material, and this fact was due to having a smaller band gap of $KOsF_3$ material than the $KRuF_3$ material. However, for the energy range of 10−22 eV both materials presented small and almost similar trend of variation in their optical conductivities curves. The highest values (16 600 unit and 12 400) of optical conductivity were seen for the $KRuF_3$ and $KOsF_3$ material to photons having energies of 24 and 23.8 eV in the UV range, respectively. The $KRuF_3$ material showed greater ability of photo conductivity than the $KOsF_3$ material in the UV range. Finally, from the results of the absorption coefficient and optical conduction in the UV energy range. Moreover, these optical properties can be tuned by the direction of electric field vector, which is also useful for designing optoelectronic materials.[31]

*Reflectivity.* The surface behaviors of both the $KRuF_3$ and $KOsF_3$ materials with the incident electromagnetic waves having a range of energies from 0 to 40 eV were also calculated and are illustrated in Figure 6d. The static values of reflectivity were observed to be 0.3 and 0.4 for the $KRuF_3$ and $KOsF_3$ compounds, respectively. It was observed that for the initial values of photon energy in the range of 0−22 eV both materials showed smaller reflection values, which indicates the transmitting behaviors of these materials surfaces to incident photons having an energy range of 0.22 eV. However, the curves of reflectivity for both the presently studied $KRuF_3$ and $KOsF_3$ materials enlarged enormously and achieved their highest values of reflectivity for the photons having energies

greater than 23.5 eV. Since the cause of reflectivity is mainly due to the available free electrons in the material, the reason for this sudden enhance in the reflectivity at this range of energies might be because of the increase in the optical conductivities of both the $KRuF_3$ and $KOsF_3$ materials at this stage of energies.

## CONCLUSIONS

The lattice constants measured for the $KRuF_3$ and $KOsF_3$ materials were found to have slight differences with each other with values of 4.24 and 4.26 Å, respectively. Moreover, the $KRuF_3$ material procures the minimal value of energy at the ground state compared to the $KOsF_3$ material and hence strengthens its capability to be more stable in the cubic structure than the $KOsF_3$ material. Both materials showed the Gold-schmidt tolerance factor ($\tau$) values and their octahedral factor ($\mu$) values in the range, which are desirable for stability of the cubic perovskite structures. Furthermore, the TDOS and PDOS patterns of the $KRuF_3$ and $KOsF_3$ materials clarified the calculated results of the band-structures of these two materials. It was found from the mechanical results of the materials that all the essential requirements, (1) $C_{11} - C_{12} > 0$, (2) $2C_{12} + C_{11} > 0$, and (3) $C_{11}$ and $C_{44} > 0$, of mechanical stability have been fulfilled by the calculated elastic constants for both the materials. Moreover, from the calculated values of the anisotropic factor ($A$) both materials were observed to have an anisotropic nature. From the optical results, it became clear that $KRuF_3$ compounds showed its greater response of absorption coefficient and optical conductivity in the UV range than the $KOsF_3$ compound.

**Computational Model.** For the comprehensive computational investigation of $KXF_3$ (where X stand for: Ru and Os) materials, we took the advantage of utilizing full potential linearized augmented plane wave method, which is based on the DFT being enforced in the WEIN2K and the electronic structures of the materials were evaluated.[32,33] Structural parameters of the material's under-consideration were determined via generalized gradient approximation and their band gaps were evaluated while pursuing the Tran and Blaha modified Becke-gradient potential.[34,35] Throughout the computational technique, the values adopted were as follows: 5 was given as the RMT (Muffin Tin Radii) value, −6 Ry was taken as cutoff energy value, $k$-points were given as 2000 ($k$-point mesh of $12 \times 12 \times 12$), and 12 (a. u)$^{-1}$ was selected as $G_{max}$ value for both the materials in the recent work. For the mechanical properties of these two materials with the cubic symmetry; IRelast package as suggested by M. Jamal integrated in WIEN2K was adopted. With the help of this package, we became enabled to get the three essential elastic constants for both the materials, which were further used to evaluate all the mechanical parameters of the studied materials. Finally, all the optical parameters needed for their use in optoelectronics and other optical devices were also evaluated in this study.

## AUTHOR INFORMATION

### Corresponding Authors

**Javed Iqbal** − *Department of Physics, Gomal University, DI Khan KP 29220, Pakistan*; Email: javedwazir86@yahoo.com

**Abid Zaman** − *Department of Physics, Riphah International University, Islamabad 44000, Pakistan*; orcid.org/0000-0001-9527-479X; Email: zaman.abid87@gmail.com

### Authors

**Jehan Y. Al-Humaidi** − *Department of Chemistry, College of Science, Princess Nourah bint Abdulrahman University, Riyadh 11671, Saudi Arabia*

**Abdullah** − *Department of Physics, Government Post Graduate College, Karak 27200, Pakistan*

**Naimat Ullah Khan** − *Department of Physics, University of Science and Technology, Bannu 28100, Pakistan*

**Shagufta Rasool** − *Department of Physics, Riphah International University, Islamabad 44000, Pakistan*

**Ali Algahtani** − *Mechanical Engineering Department, College of Engineering, King Khalid University, Abha 61421 Asir, Kingdom of Saudi Arabia; Research Center for Advanced Materials Science (RCAMS), King Khalid University, Abha 61413 Asir, Kingdom of Saudi Arabia*

**Vineet Tirth** − *Mechanical Engineering Department, College of Engineering, King Khalid University, Abha 61421 Asir, Kingdom of Saudi Arabia; Research Center for Advanced Materials Science (RCAMS), King Khalid University, Abha 61413 Asir, Kingdom of Saudi Arabia;* orcid.org/0000-0002-8208-7183

**Altaf Ur Rahman** − *Department of Physics, Riphah International University, Lahore 54000, Pakistan;* orcid.org/0000-0001-7772-3272

**Barno Sayfutdinovna Abdullaeva** − *Professor, Doctor of Pedagogical Sciences, Vice-Rector for Scientific Affairs, Tashkent State Pedagogical University, Tashkent 100027, Uzbekistan*

**Moamen S. Refat** − *Department of Chemistry, College of Science, Taif University, Taif 21944, Saudi Arabia*

**Muhammad Aslam** − *Institute of Physics and Technology, Ural Federal University, Yekaterinburg 620002, Russia*

Complete contact information is available at:
https://pubs.acs.org/10.1021/acsomega.3c03810

### Notes

The authors declare no competing financial interest.

## ACKNOWLEDGMENTS

## REFERENCES

(1) Kojima, A.; Teshima, K.; Shirai, Y.; Miyasaka, T. Organometal halide perovskites as visible-light sensitizers for photovoltaic cells. *J. Am. Chem. Soc.* **2009**, *131* (17), 6050−6051.

(2) Deschler, F.; Price, M.; Pathak, S.; Klintberg, L. E.; Jarausch, D. D.; Higler, R.; Hüttner, S.; Leijtens, T.; Stranks, S. D.; Snaith, H. J.; et al. High photoluminescence efficiency and optically pumped lasing in solution-processed mixed halide perovskite semiconductors. *J. Phys. Chem. Lett.* **2014**, *5* (8), 1421−1426.

(3) Glushkova, A.; Andricevic, P.; Smajda, R.; Náfrádi, B.; Kollar, M.; Djokic, V.; Arakcheeva, A.; Forró, L.; Pugin, R.; Horváth, E. Ultrasensitive 3D aerosol-jet-printed perovskite X-ray photodetector. *ACS Nano* **2021**, *15* (3), 4077−4084.

(4) Tiguntseva, E. Y.; Zograf, G. P.; Komissarenko, F. E.; Zuev, D. A.; Zakhidov, A. A.; Makarov, S. V.; Kivshar, Y. S. Light-emitting halide perovskite nanoantennas. *Nano Lett.* **2018**, *18* (2), 1185−1190.

(5) Sichert, J. A.; Tong, Y.; Mutz, N.; Vollmer, M.; Fischer, S.; Milowska, K. Z.; García Cortadella, R.; Nickel, B.; Cardenas-Daw, C.; Stolarczyk, J. K.; et al. Quantum size effect in organometal halide perovskite nanoplatelets. *Nano Lett.* **2015**, *15* (10), 6521−6527.

(6) Chen, M.; Yang, J.; Wang, Z.; Xu, Z.; Lee, H.; Lee, H.; Zhou, Z.; Feng, S.; Lee, S.; Pyo, J.; et al. Perovskite Nanoprinting: 3D Nanoprinting of Perovskites (Adv. Mater. 44/2019). *Adv. Mater.* **2019**, *31* (44), 1970310.

(7) Chen, M.; Hu, S.; Zhou, Z.; Huang, N.; Lee, S.; Zhang, Y.; Cheng, R.; Yang, J.; Xu, Z.; Liu, Y.; et al. Three-dimensional perovskite nanopixels for ultrahigh-resolution color displays and multilevel anticounterfeiting. *Nano Lett.* **2021**, *21* (12), 5186−5194.

(8) Kubicek, M.; Bork, A. H.; Rupp, J. L. Perovskite oxides—a review on a versatile material class for solar-to-fuel conversion processes. *J. Mater. Chem. A* **2017**, *5* (24), 11983−12000.

(9) Pandey, R.; Vats, G.; Yun, J.; Bowen, C. R.; Ho-Baillie, A. W.; Seidel, J.; Butler, K. T.; Seok, S. I. Mutual insight on ferroelectrics and hybrid halide perovskites: a platform for future multifunctional energy conversion. *Adv. Mater.* **2019**, *31* (43), 1807376.

(10) Yin, W. J.; Weng, B.; Ge, J.; Sun, Q.; Li, Z.; Yan, Y. Oxide perovskites, double perovskites and derivatives for electrocatalysis, photocatalysis, and photovoltaics. *Energy Environ. Sci.* **2019**, *12* (2), 442−462.

(11) Iqbal, J.; Liu, H.; Hao, H.; Ullah, A.; Cao, M.; Yao, Z.; Manan, A. Mg (Ti0. 95Sn0. 05) O3−(Ca0. 8Sr0.2) TiO3 ceramics: Phase, microstructure, and microwave dielectric properties. *J. Alloys Compd.* **2018**, *742*, 107−111.

(12) Tian, L.; Hu, Z.; Liu, X.; Liu, Z.; Guo, P.; Xu, B.; Xue, Q.; Yip, H. L.; Huang, F.; Cao, Y. Fluoro-and amino-functionalized conjugated polymers as electron transport materials for perovskite solar cells with improved efficiency and stability. *ACS Appl. Mater. Interfaces* **2019**, *11* (5), 5289−5297.

(13) Rashid, M. Study of Vanadium Difluoride AVF3 (A= Na, K, Rb) for Optoelectronic and Thermoelectric Device Applications via Ab Initio Calculations. *J. Supercond. Novel Magn.* **2020**, *33* (4), 1167−1175.

(14) Guo, Y.; Kee Moon, B.; Heum Park, S.; Hyun Jeong, J.; Hwan Kim, J.; Jang, K.; Yu, R. A red-emitting perovskite-type SrLa(1−)-MgTaO6:xEu3+ for white LED application. *J. Lumin.* **2015**, *167*, 381−385.

(15) Ihringer, J.; Maichle, J. K.; Prandl, W.; Hewat, A. W.; Wroblewski, T. Crystal structure of the ceramic superconductor BaPb 0.75 Bi 0.25 O 3. *Z. Phys. B: Condens. Matter* **1991**, *82*, 171−176.

(16) Oleaga, A.; Salazar, A.; Skrzypek, D. Critical behaviour of magnetic transitions in KCoF3 and KNiF3 perovskites. *J. Alloys Compd.* **2015**, *629*, 178−183.

(17) Ohno, H.; Shen, A.; Matsukura, F.; Oiwa, A.; Endo, A.; Katsumoto, S.; Iye, Y. (Ga, Mn) As: a new diluted magnetic semiconductor based on GaAs. *Appl. Phys. Lett.* **1996**, *69* (3), 363−365.

(18) Rashid, M. Study of Vanadium Difluoride AVF3 (A= Na, K, Rb) for Optoelectronic and Thermoelectric Device Applications via Ab Initio Calculations. *J. Supercond. Novel Magn.* **2020**, *33* (4), 1167−1175.

(19) Abdullah; Khan, U. A.; Khan, S.; Ahmed, S. J.; Khan, N. U.; Ullah, H.; Naz, S.; Farhat, L. B.; Amami, M.; Tirth, V.; et al. Structural, Electronic and Optical Properties of Titanium Based Fluoro-Perovskites MTiF3 (M= Rb and Cs) via Density Functional Theory Computation. *ACS Omega* **2022**, *7* (51), 47662−47670.

(20) Chenine, D.; Aziz, Z.; Benstaali, W.; Bouadjemi, B.; Youb, O.; Lantri, T.; Abbar, B.; Bentata, S. Theoretical Investigation of Half-Metallic Ferromagnetism in Sodium-Based Fluoro-perovskite NaXF3 (X= V, Co). *J. Supercond. Novel Magn.* **2018**, *31* (1), 285−295.

(21) Bartel, C. J.; Sutton, C.; Goldsmith, B. R.; Ouyang, R.; Musgrave, C. B.; Ghiringhelli, L. M.; Scheffler, M. New tolerance factor to predict the stability of perovskite oxides and halides. *Sci. Adv.* **2019**, *5* (2), No. eaav0693.

(22) Al-Humaidi, J. Y.; Ullah, A.; Khan, N. U.; Iqbal, J.; Khan, S.; Algahtani, A.; Tirth, V.; Al-Mughanam, T.; Refat, M. S.; Zaman, A.

First-principle insight into the structural, electronic, elastic and optical properties of Cs-based double perovskites Cs 2 XCrCl 6 (X= K, Na). *RSC Adv.* **2023**, *13* (30), 20966−20974.

(23) Togo, A.; Oba, F.; Tanaka, I. First-principles calculations of the ferroelastic transition between rutile-type and CaCl 2-type SiO 2 at high pressures. *Phys. Rev. B* **2008**, *78* (13), 134106.

(24) Ayaz Khan, U.; Sarker, M. R.; Sarker, M. R.; Khan, N. U.; Khan, S.; Al-Humaidi, J. Y.; Tirth, V.; Refat, M. S.; Zaman, A.; Algahtani, A.; et al. Investigation of structural, opto-electronic, mechanical and thermoelectric properties of Rb-based fluoro-perovskites RbXF3 (X= Rh, Os, Ir) via first-principles calculations. *J. Saudi Chem. Soc.* **2023**, *27* (3), 101627.

(25) Yang, Y.; Wang, J.; Liu, Y.; Cui, Y.; Ding, G.; Wang, X. Topological phonons in Cs-Te binary systems. *Phys. Rev. B* **2023**, *107* (2), 024304.

(26) Sajjad, M.; Sajjad, M.; Khan, U. A.; Ullah, H.; Alhodaib, A.; Amami, M.; Tirth, V.; Zaman, A.; Shazia. Structural, electronic, magnetic and elastic properties of xenon-based fluoroperovskites XeMF 3 (M= Ti, V, Zr, Nb) via DFT studies. *RSC Adv.* **2022**, *12* (42), 27508−27516.

(27) Yang, Y.; Lu, H.; Yu, C.; Chen, J. M. First-principles calculations of mechanical properties of TiC and TiN. *J. Alloys Compd.* **2009**, *485* (1−2), 542−547.

(28) Jamil, M. T.; Ahmad, J.; Bukhari, S. H.; Sultan, T.; Akhter, M. Y.; Ahmad, H.; Murtaza, G. Effect on structural and optical properties of Zn-substituted cobalt ferrite CoFe2O4. *J. Ovonic Res.* **2017**, *13* (1), 45−53.

(29) Bhattacharya, B.; Deb, J.; Sarkar, U. Boron-phosphorous doped graphyne: a near-infrared light absorber. *AIP Adv.* **2019**, *9* (9), 095031.

(30) Khan, U. A.; Khan, N. U.; Alghtani, A. H.; Alghtani, A. H.; Tirth, V.; Ahmed, S. J.; Sajjad, M.; Algahtani, A.; Shaheed, T.; Zaman, A. First-principles investigation on the structural, electronic, mechanical and optical properties of silver based perovskite AgXCl3 (X= Ca, Sr). *J. Mater. Res. Technol.* **2022**, *20*, 3296−3305.

(31) Deb, J.; Sarkar, U. Boron-nitride and boron-phosphide doped twin-graphene: Applications in electronics and optoelectronics. *Appl. Surf. Sci.* **2021**, *541*, 148657.

(32) Gao, S.; Hahn, J. R.; Ho, W. Adsorption induced hydrogen bonding by CH group. *J. Chem. Phys.* **2003**, *119* (12), 6232−6236.

(33) Schwarz, K. DFT calculations of solids with LAPW and WIEN2k. *J. Solid State Chem.* **2003**, *176* (2), 319−328.

(34) Blaha, P. *WIEN2k: An Augmented Plane Wave Plus Local Orbitals Program for Calculating Crystal Properties*; Techn.Universitat, 2018.

(35) Tran, F.; Blaha, P. Accurate band gaps of semiconductors and insulators with a semilocal exchange-correlation potential. *Phys. Rev. Lett.* **2009**, *102* (22), 226401.